ORGANIC LETTERS

2007
Vol. 9, No. 15
2803−2806

# The Element Effect in Nucleophilic Aromatic Photosubstitution ($S_N2Ar^*$)

**Gene G. Wubbels,* Kandra M. Johnson, and Travis A. Babcock**

*Department of Chemistry, University of Nebraska at Kearney, Kearney, Nebraska 68849*

*wubbelsg@unk.edu*

**Received April 18, 2007**

## ABSTRACT

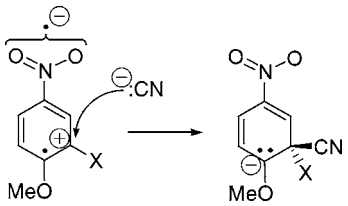


**Photoreactions of 4-nitroanisole and the 2-halo-4-nitroanisoles (halogen = F, Cl, Br, I) with NaCN have been investigated. 4-Nitroanisole gave a novel, stable nitronate ion adduct (74%) with cyanide. For the five compounds, we report product distributions, Stern–Volmer kinetic plots, triplet lifetimes, and triplet yields, which afford rate constants for attack by the cyanide ion. Cyanide attack on the fluoride is diffusion controlled; the relative rates for attack at F, Cl, Br, and I are 27:2:2:1, respectively.**

The element effect,[1] particularly that of the halogens, has played a fundamental role in resolving mechanisms in organic chemistry. Quantitative evidence of the effect was central in understanding aliphatic substitution and elimination reactions[2] and nucleophilic aromatic substitutions of the $S_N$-2Ar type.[3,4] The element effect for nucleophilic aromatic photosubstitutions of the $S_N2Ar^*$ type, reactions whose mechanisms[5] and applications[6,7] have been widely studied, has not been established. We sought to remedy this deficiency to answer some basic questions about the transition state: (1) is the element effect dominated by leaving group effects as in thermal aliphatic substitutions and eliminations (F ≪ Cl < Br < I) or by $\sigma$-bond polarization and steric effects as in thermal nucleophilic aromatic substitution (F ≫ Cl > Br > I)? and (2) does the fastest nucleophile-dependent reaction from the triplet state in this graded series show a rate constant slowed by spin forbiddenness in the formation of the singlet $\sigma$-bonded intermediate?

The photoreaction of 4-nitroanisole (**1**) with the cyanide ion in mixed aqueous media was reported by Letsinger and co-workers,[8] who found products resulting from bond formation by the cyanide ion meta to the nitro group and a nitrite displacement product. They also reported an intensely absorbing stable intermediate of unknown structure ($\lambda_{max}$ 364 nm in 20% *t*-butyl alcohol−water) when the photolysis solution was free of oxygen. When we irradiated **1** (0.0060 M) in oxygen-free 40% DMSO-$d_6$−$D_2O$ (v/v) or 33% $CD_3CN$−$D_2O$ (v/v) containing 0.020 M NaCN in a borosilicate NMR tube at 313 nm at 0 or 35 °C, we found NMR evidence for two photoproducts (**2** and **3**) that accounted for 26% and 74%, respectively, of the reacted starting material. The results appear in Scheme 1. Compound **2** was expected[8b] and was confirmed by enhancement of its NMR signals with an authentic sample. The structure of nitronate ion **3** was inferred from its spectra. It showed $\lambda_{max}$ 371 nm ($\epsilon \approx 13\,000$) in 33% $CH_3CN$−$H_2O$ and $^1H$ NMR signals (33% $CD_3CN$−

(1) Mueller, P. *Pure Appl. Chem.* **1994**, *66*, 1077.
(2) Lowry, T. H.; Richardson, K. S. *Mechanism and Theory in Organic Chemistry*, 3rd ed.; Harper & Row: New York, 1987; p 374.
(3) Bunnett, J. F.; Garbisch, E. W.; Pruitt, K. M. *J. Am. Chem. Soc.* **1957**, *79*, 385.
(4) Bordwell, F. G.; Hughes, D. L. *J. Am. Chem. Soc.* **1986**, *108*, 5991.
(5) Karapire, C.; Icli, S. In *Organic Photochemistry and Photobiology*, 2nd ed.; Horspool, W., Lenci, F., Eds.; CRC Press: Boca Raton, 2004; Chapter 37, pp 37-1−37-14.
(6) Specht, A.; Goeldner, M. *Angew. Chem., Int. Ed.* **2004**, *43*, 2008.
(7) Schutt, L.; Bunce, N. J. In *Organic Photochemistry and Photobiology*, 2nd ed.; Horspool, W., Lenci, F., Eds.; CRC Press: Boca Raton, 2004; Chapter 38, pp 38-1−38-18.
(8) (a) Letsinger, R. L.; McCain, J. H. *J. Am. Chem. Soc.* **1969**, *91*, 6425. (b) Letsinger, R. L.; Hautala, R. R. *Tetrahedron Lett.* **1969**, 4205.

10.1021/ol070910m CCC: $37.00 
**Published on Web 06/30/2007**

**Scheme 1.** Photoproducts of **1** with the Cyanide Ion under Air-Free Conditions

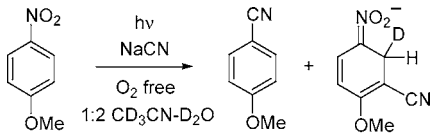


**1** **2** **3**

$D_2O$) as follows (shifts relative to $CD_2HCN$ at $\delta$ 2.03): $\delta$ 6.56, 1H, d ($J$ = 5.7 Hz); $\delta$ 6.11, 1H, d ($J$ = 5.7 Hz); $\delta$ 3.79, 3H, s; $\delta$ 3.70, 1H, br s. When the solution of **2** and **3** was mixed at 25 °C with 3,5-dinitrobenzoic acid, a substance known to oxidize dihydrobenzenes to benzenes,[9] the NMR signals of **3** were replaced by those of 2-methoxy-5-nitrobenzonitrile having the C-6 position about 80% deuterated. A likely pathway to **3** involves making a strongly basic $\sigma$-complex by meta attack of cyanide on photoexcited **1**, capture of a deuteron by the $\sigma$-complex to make a dihydrobenzene, and loss of a vinylogous alkyl nitro proton ($pK_a \cong 7$).

The photolyses of **1** and the 2-halo-4-nitroanisoles (**4** (2-F), **5** (2-Cl), **6** (2-Br), and **7** (2-I)) were carried out typically at 0.0030 M with 0.010 M NaCN in oxygen-free 33% $CD_3CN-D_2O$ (v/v) in borosilicate NMR tubes at ca. 35 °C with unfiltered broad-band light from 300 nm lamps (Rayonet RPR-208). The analyses relied mostly on the integrations of the methoxy singlets that showed baseline separations at 300 MHz in the range of 4.0 to 3.6 $\delta$. Replacement of halogen by cyanide was the major reaction for **4**−**7**, giving in all cases 2-methoxy-5-nitrobenzonitrile, whose methoxy peak is downfield 0.06 ppm from those of the starting materials. Its spectrum was confirmed with an authentic sample. A minor product resulted from nitro group displacement by cyanide, which gave a 0.06 ppm upfield-shifted methoxy signal relative to starting material in all cases. The spectrum of this minor product from the bromide was confirmed with an authentic sample. The other minor product was the cyanide nitronate adduct analogous to **3**, which showed in all cases a substantially upfield-shifted methoxy signal. This was confirmed for the chloride by oxidizing the solution containing the nitronate with 3,5-dinitrobenzoic acid, which caused the spectrum of 2-methoxy-3-chloro-5-nitrobenzonitrile to appear (deuterated at C-6). The product distributions were measured in duplicate at 20−40% conversion. Results are given in Table 1.

Stern−Volmer plots of reciprocal quantum yield vs reciprocal cyanide ion concentration were acquired with samples ($2.0 \times 10^{-4}$ M) in quartz cuvettes in oxygen-free 33% $CH_3CN-H_2O$ (v/v) with NaCN at 0.020−0.0010 M. Cyanide ion concentrations were corrected for hydrolysis as if they were in pure water. Irradiation was at 313 nm obtained with a chromate filter from broad-band 300 nm lamps. Photoreactions were followed by overlaid UV scans to find

**Table 1.** Product Percent Yields from Cyanide Photoreactions

| reactant | 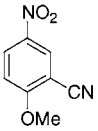 | 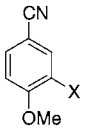 | 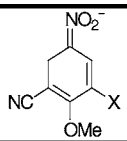 |
|---|---|---|---|
| 4-nitroanisole | -- | 26% | 74% |
| 2-fluoro-4-nitroanisole | 88% | 9% | 3% |
| 2-chloro-4-nitroanisole | 61% | 29% | 10% |
| 2-bromo-4-nitroanisole | 57% | 32% | 11% |
| 2-iodo-4-nitroanisole | 48% | 43% | 9% |

a monitoring wavelength. Reactions were clean as shown by sharp isosbestic points and linear fraction of reaction with irradiation time through 10% reaction. The reaction extent was measured between 5 and 10% conversion; the actinometer was azoxybenene in ethanol.[10] Plots of $1/\Phi$ vs $1/[CN^-]$ were linear with correlation coefficients greater than 0.98. The slopes, intercepts, and limiting quantum yields at extrapolated infinite cyanide ion concentration are given in Table 2.

**Table 2.** Stern−Volmer Kinetics for Photoreactions of Nitroanisoles with the Cyanide Ion

| reactant | slope | intercept | intercept$^{-1}$ ($\Phi_{lim}$) |
|---|---|---|---|
| 4-nitroanisole | 0.020 | 1.6 | 0.62 |
| 2-fluoro-4-nitroanisole | 0.0023 | 1.6 | 0.62 |
| 2-chloro-4-nitroanisole | 0.024 | 3.0 | 0.34 |
| 2-bromo-4-nitroanisole | 0.029 | 5.6 | 0.18 |
| 2-iodo-4-nitroanisole | 0.246 | 62 | 0.016 |

Triplet lifetimes and yields were obtained in oxygen-free 33% $CH_3CN-H_2O$ through use of a nanosecond transient spectrometer using 8 ns pulses at 355 nm. The triplet−triplet absorption maximum was found at 400 ± 10 nm and was used to monitor decay. The maximum optical density (O.D.) at the origin of the transient allowed estimation of the triplet yield with the assumptions that the triplet−triplet extinction coefficient was constant for each of the five compounds and that the largest absorbance (for the chloride) corresponded to a triplet yield of 0.90. These results are given in Table 3.

A plausible mechanistic scheme for this reaction system is given in Scheme 2. The production of **3** in high yield from **1** suggests that the cyano−carbon bond in any $\sigma$-complex does not break appreciably and that decay of the $\sigma$-complexes

(9) Wubbels, G. G.; Halverson, A. M.; Oxman, J. D.; DeBruyn, V. H. *J. Org. Chem.* **1985**, *50*, 4499.

(10) Bunce, N. J.; LaMarre, J.; Vaish, S. P. *Photochem. Photobiol.* **1984**, *39*, 531.

**Table 3.** Triplet Lifetimes, Decay Constants, and Triplet Yields for Nitroanisoles

| compound | lifetime (ns ± s.d.) | $k_d$ ($s^{-1}$) | T-T max O.D. at 400 nm | $\Phi_{ISC}$ |
|---|---|---|---|---|
| 4-nitroanisole | 58 ± 3 | $1.7 \times 10^7$ | 0.053 | 0.69 |
| 2-fluoro-4-nitroanisole | 217 ± 6 | $4.6 \times 10^6$ | 0.048 | 0.62 |
| 2-chloro-4-nitroanisole | 137 ± 12 | $7.4 \times 10^6$ | 0.069 | 0.90 |
| 2-bromo-4-nitroanisole | 116 ± 1.3 | $8.6 \times 10^6$ | 0.064 | 0.84 |
| 2-iodo-4-nitroanisole | 44.5 ± 0.4 | $2.2 \times 10^7$ | 0.031 | 0.40 |

**Scheme 2.** Photoreactions of Nitroanisoles with the Cyanide Ion

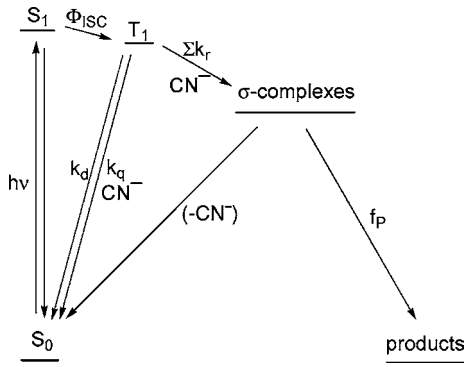


to starting material by loss of the cyanide ion is negligible. This implies that the fraction of $\sigma$-complexes making products is unity ($f_P = 1$). With this assumption, eqs 1−3 can be readily derived.

$$\frac{1}{\Phi_X} = \frac{1}{\Phi_{ISC}}\left(1 + \frac{k_q}{\sum k_r} + \frac{k_d}{\sum k_r[CN^-]}\right) \quad (1)$$

$$\text{slope} = \frac{1}{\Phi_{ISC}}\left(\frac{k_d}{\sum k_r}\right) \Rightarrow \sum k_r = \frac{1}{\Phi_{ISC}}\left(\frac{k_d}{\text{slope}}\right) \quad (2)$$

$$\text{intercept} = \frac{1}{\Phi_{ISC}}\left(1 + \frac{k_q}{\sum k_r}\right) \quad (3)$$

Equation 1 predicts the linear Stern−Volmer plots, and the values from Tables 2 and 3 allow calculation of $\sum k_r$ and $k_q$. The individual rate constants in $\sum k_r$ can be extracted from the sum with the assumption that the product yields in Table 1 are proportional to the nucleophilic attack rate constants that give their precursor $\sigma$-complexes. Rate constants for several of the elementary processes of this system are given in Table 4.

These numbers disclose reassuring regularity and interesting differences with changes in the halogen substituent. The nitro group displacement ($k_{nitro}$) would be expected to be little affected by the meta substituent, and indeed the rate constants are within a factor of 3. Similarly, the rates of bond formation at the unsubstituted *meta*-carbon would be expected to be modestly affected by halogens at the meta position, and they

**Table 4.** Rate Constants of Cyanide Ion Processes with Triplet Nitroanisoles

| reactant | $\sum k_r$ $10^9$ $M^{-1}s^{-1}$ | $k_q$ $10^9$ $M^{-1}s^{-1}$ | $k_{nitro}$ $10^9$ $M^{-1}s^{-1}$ | $k_{m-C}$ $10^9$ $M^{-1}s^{-1}$ | $k_X$ $10^9$ $M^{-1}s^{-1}$ |
|---|---|---|---|---|---|
| 1 | 1.2 | 0.15 | 0.29 | 0.89 | n.a. |
| 4 | 3.3 | 0.011 | 0.29 | 0.081 | 2.9 |
| 5 | 0.34 | 0.56 | 0.098 | 0.034 | 0.21 |
| 6 | 0.36 | 1.3 | 0.11 | 0.039 | 0.20 |
| 7 | 0.22 | 5.4 | 0.096 | 0.020 | 0.11 |

are within a factor of 4. That this rate constant for **1** is about 10 times greater than that of **4** may reflect its statistical advantage of two meta positions and other unknown effects of having no halogen on the ring. The ratio of rate constants for nitro vs *meta*-carbon attack is quite steady for the halogen series, as would be expected. Because the nucleophile-induced quenching mechanism is unknown, we do not interpret these rate constants except to note that they correlate with the polarizability expected for the compounds. The quenching of the iodide is very fast and accounts for the great inefficiency of its product formation ($\Phi_{lim} = 0.016$). This contrasts with the fluoride, which shows slow quenching and whose net limiting quantum yield ($\Phi_{lim} = 0.62$) is the same as the estimated quantum yield of intersystem crossing.

The rate constants for the attack of the cyanide ion at the halogen-bearing carbons are of primary interest. The rate for the fluoride is at the diffusion limit, which for water is reported for non-lyate reactants having no ionic attraction or repulsion to be $3 \times 10^9$ $M^{-1}$ $s^{-1}$.[11] The rate ratios for F:Cl:Br:I are 27:2:2:1, respectively. These follow the pattern of aromatic substitution and not aliphatic substitution or elimination, implying that carbon−nucleophile bond formation not carbon−halogen bond fission is the principal efficiency-determining process.

An analogous thermal nucleophilic aromatic substitution of 1-halo-4-nitrobenzenes with sodium methoxide in methanol shows relative rates of halogen displacement of 1300:3:2:1 for F:Cl:Br:I, respectively, the iodide having a rate constant of $1.3 \times 10^{-7}$ $M^{-1}$ $s^{-1}$.[12] If the photoreaction of the fluoride is indeed diffusion controlled, the intrinsic energy barrier of the reaction is zero, and the incremental barriers for Cl, Br, and I are 1.6, 1.6, and 1.9 kcal/mol. The increments of Arrhenius activation energy for the thermal displacements relative to the fluoride are (for Cl, Br, and I) 3.6, 3.8, and 4.2 kcal/mol. Despite absolute rate differences on the order of $10^{14}$, the two reaction series show comparable halogen element effects and barrier increments. This suggests that, despite vast differences, the photoreaction, like the thermal one, must involve simple electron-paired bond formation with its attendant van der Waals repulsion and $\sigma$-bond polarization effects of the attached halogen.

Attempts to understand the $S_N2Ar^*$ mechanism proceeding from a $\pi,\pi^*$ excited state have a long history.[13] Two current

(11) (a) Eigen, M. *Angew. Chem., Int. Ed.* **1964**, *3*, 1. (b) Weller, A. *Z. Physik. Chem.* **1958**, *17*, 224.
(12) Bartoli, G.; Todesco, P. E. *Acc. Chem. Res.* **1977**, *10*, 125.
(13) Cornelisse, J.; Havinga, E. *Chem. Rev.* **1975**, *75*, 353.

**Scheme 3.** Transition State for Reaction of a Nucleophile and a Triplet $\pi,\pi^*$ State to Make a $\sigma$-Complex Directly

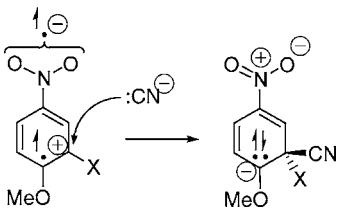


theories[14,15] rationalize the predominant regiochemistry of these reactions, including those reported here, but neither illuminates formation of the $\sigma$-complexes that both assume. That the fluoride $\sigma$-complex forms at the rate of diffusion means that there is no reaction energy barrier and no spin forbiddenness. That halogen substituents confer almost the same effects as in the thermal reaction means that the geometric and local electronic structures of the thermal and photochemical transition states are similar. We envision this as shown in Scheme 3. The first structure is a modified valence bond depiction of the $\pi,\pi^*$ excited state of a halonitroanisole showing the electron hole mainly in the $\pi$ orbitals of the ring and the promoted electron in an antibonding orbital mainly on the nitro group. Electron-paired bond formation must cause the system to enter a funnel in the potential energy surfaces that leads ineluctably to spin inversion and electron demotion. This is analogous to a recently discovered electron-paired nucleophilic reaction of a *para*-benzyne biradical.[16]

**Acknowledgment.** Acknowledgment is made to the donors of the Petroleum Research Fund, administered by the American Chemical Society, for support of this work. We thank Amy Vega and Prof. Michael Wasielewski of Northwestern University for the transient measurements.

**Supporting Information Available:** $^1$H NMR spectra for Scheme 1 and Table 1, Stern−Volmer plots for Table 2, and a typical decay curve for Table 3. This material is available free of charge via the Internet at http://pubs.acs.org.

OL070910M

(14) Epiotis, N. D.; Shaik, S. *J. Am. Chem. Soc.* **1978**, *100*, 29.
(15) van Riel, H. C. H. A.; Lodder, G.; Havinga, E. *J. Am. Chem. Soc.* **1981**, *103*, 7257.
(16) Perrin, C. L.; Rodgers, B. L.; O'Connor, J. M. *J. Am. Chem. Soc.* **2007**, *129*, 4795.